Assessing the Environmental Performance of BIPV Systems under Different Environmental Conditions

Aanuoluwapo Aderonke Oguntade[1] and Marco Cimillo [1*]

[1] Xi'an Jiaotong-Liverpool University
marco.cimillo@xjtlu.edu.cn

Abstract. This paper provides an overview of Building-Integrated Photovoltaic (BIPV) environmental performance in different conditions. Four different technologies were selected based on their representativeness of the currently available systems and on the availability of the necessary data. Their characteristics, including lifespan, efficiency, and embodied energy and carbon, were identified through a database search and a review of recently published research. The energy production was estimated assuming the installation of the systems on the optimal orientation, a flat roof and façades facing due to the four cardinal directions. The simulation considered ten locations in different climates and with different solar irradiations and climates. The final environmental performance is calculated based on energy and CO_2 balance, mainly through the Energy Payback Time (EPBT), Carbon Payback Time (CPBT) and Carbon Intensity (CI). Although limited by the assumptions and simplifications necessary to conduct a wide-ranging study, the paper offers a representative dataset and insights into the viability of the main currently available BIPV solutions in different climatic regions.

Keywords: building integrated photovoltaic, energy payback time, carbon payback time, carbon intensity.

1 Introduction

Roughly 25 per cent of greenhouse gas emissions and 33 per cent of the world's energy consumption are attributable to the building sector (González-Torres et al., 2022). By 2050, the global population is predicted to reach 9.7 billion people (United Nations Department of Economic and Social Affairs, Population Division, 2022), and as the population grows, so does the energy demand. There is a need for sustainable energy alternatives that are closer to the consumers to meet the projected increase in energy demand (Muteri et al., 2020). Therefore, it is unsurprising that the number of publications on building integrated photovoltaics (BIPV) has increased in the past 36 years (Kant Paliwal et al., 2024). There are several research publications on how to improve the energy performance and efficiency of BIPVs and how BIPVs influence the performance of buildings (building energy demand and users' comfort). Numerous

W. Guo et al. (eds.), *Proceedings of the 3rd International Conference on Green Building, Civil Engineering and Smart City (GBCESC 2024)*, Advances in Engineering Research 264,
https://doi.org/10.2991/978-94-6463-728-1_49

studies also address the urban application of BIPVs, their life cycle assessment (LCA) and environmental impact.

Nonetheless, there are still significant gaps to be filled on the LCA of BIPV, particularly in terms of the environmental impact of BIPV across different geographical regions. The location, timing, and nature of the BIPV project all influence the conclusions of LCA studies. Also, LCA results are often only valid for a certain number of years because the relevant factors constantly change as manufacturers upgrade systems and processes. Thus, the LCA for BIPV is an evergreen topic of interest. After conducting a systematic search in the Web of Science and Scopus database on publications on the life cycle assessment of BIPVs, it was observed that the recent review journal publications on the LCA of BIPVs consolidated findings on the energy payback time (EPBT) and global warming potential (GWP) of BIPV systems from works published more than five years ago, which may not be representative of the current values and therefore need an update. This study aims to overcome this gap by calculating the EPBT, carbon payback time (CPBT), and carbon intensity (CI) of various PV technologies for 10 study locations, assuming they are positioned optimally, horizontally integrated into the roof and vertically spaced on the façade facing the four cardinal points.

Calculating the EPBT, CPBT, and CI of photovoltaic (PV) systems in a particular location helps determine if investing in PV is justifiable from an environmental perspective compared to the existing energy alternatives in such places. Also, calculating the EPBT, CPBT, and CI of PV systems in different placements helps to provide helpful information on which building integration placement is most environmentally friendly, thus avoiding the suboptimal placement of PV panels. The issue of CPBT of PV panels will become more relevant in the years to come. Already, Sweden pioneered the climate declaration policy, which requires that the greenhouse gas (GHG) emissions associated with the construction phase of building projects be declared (von Malmborg, 2024). Integrating PV systems into buildings would impact the GHG emissions of buildings and their embodied carbon as well. Therefore, there is a need to study the CI of BIPV systems. The outcomes of this research will help investors, developers, and other stakeholders, including policymakers, to make insightful decisions.

2 Methodology

Ten locations were selected to examine the EPBT and CPBT of different solar PV technologies under different solar irradiation conditions. Fig. 1. shows the global horizontal irradiation globally, with annual values ranging from around 750 kWh/m^2 to 2750 kWh/m^2. For this research, locations were selected around each of the following intervals: 750, 1000, 1250, 1500, 1750, 2000, 2250, 2500 and 2750 kWh/m^2. The PVGIS website was used to identify the coordinates of the study locations whose annual solar irradiation per meter square fell within the chosen interval; it was also used to determine the optimal PV panel slope and azimuth for each site. Photovoltaic energy production is also function of other climatic variables, including air temperature, which affects the modules' temperature and their efficiency. Therefore, the study locations are to be representative of different geographical and climatic regions. At least one location was selected from the very hot, hot, warm, mixed, cool, cold and very cold climatic region from the ASHRAE thermal zone classification. The extremely hot and arctic regions are excluded as applications are limited. Locations belong to countries with varied carbon intensity of grid electricity, from as little as 0.03 kg CO_2e /kWh in Norway to as high as 0.71 kg CO_2e /kWh in China. Thus, the study provides a dataset representative of a comprehensive range of technologies and environmental conditions. Four PV panel technologies, two from the first generation and two from the second generation, were used to determine the EPBT: monocrystalline, polycrystalline, cadmium telluride, and copper indium gallium selenide. Only cadmium telluride and copper indium gallium selenide were selected from the second generation of PV panel technology because of the availability of current data on their embodied energy and embodied carbon.

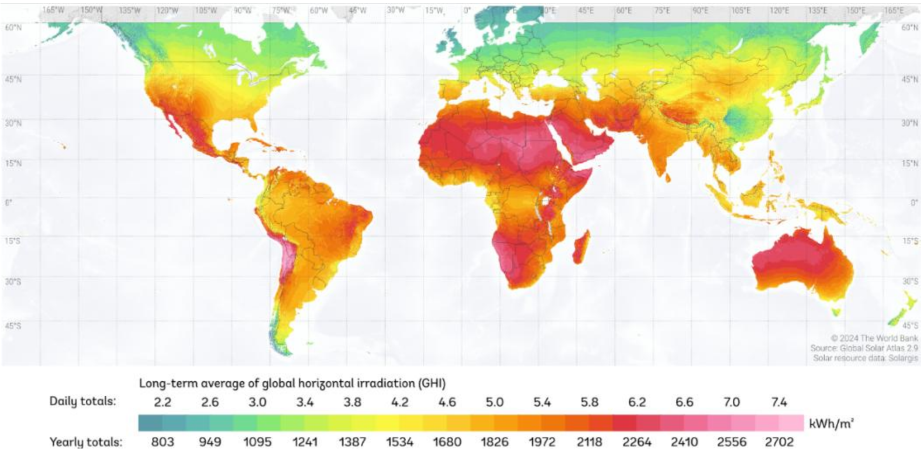

Fig. 1. Global horizontal irradiation (GHI) (Global Solar Atlas 2.0, 2020).

Data on the embodied energy of the monocrystalline and polycrystalline PV panels were obtained from the Environmental Product Declarations (EPDs) obtained from the One Click LCA database. The embodied energy for the cadmium telluride and copper indium gallium selenide panels was obtained from published research as their EPDs were unavailable in the One Click LCA database. The mounting system and the balance of system (BOS), which includes inverters, electric cables, circuit breakers, and electric meters, were captured in this study through data from the One Click LCA database. The embodied energy of the 'Mono-Si - SPR-MAX3-400' PV panel was 1838.62 MJ/m^2 (SunPower, 2021), and for the 'Poly-Si - JAP6-60-280/4BB/RE', it was 2309.59 MJ/m^2 (JA SOLAR, 2019). According to (Wikoff et al., 2022), the embodied energy of a cadmium telluride PV panel was 762 MJ/m^2, and according to (Stamford & Azapagic, 2019), the embodied energy of one copper indium gallium selenide panel (141WP/ 0.939m^2) was 126 MJ. Care was taken to use EPDs and data not older than five years, to ensure the results are up to date.

This study did not include the energy used in transporting the PV panels and BOS to the project site, for installation and for disposal or recycling in the EPBT calculations. A 3 kWp inverter capacity was assumed; as such, the PV panels were sized to be a little below the inverter capacity (see Table 1 for the details). To attain the desired PV capacity, seven, ten, six and seventeen numbers of the monocrystalline, polycrystalline, cadmium telluride and copper indium gallium selenide PV panels, respectively, were used. The energy production for the identified coordinates was estimated using RETScreen clean energy management software with the assumption that the PV panels were placed in the optimal position, horizontally on a flat roof and vertically on façades facing the four cardinal directions. It was also assumed that the PV panels were not shaded in their respective positions to provide the bases for comparing the results across all the study locations This setting is designed to compare the selected technologies in different climatic and energy contexts, not to evaluate specific building sites or architectural configurations. The EPBT was calculated using Equation 1 without taking into account the annual degradation rate of the PV panels.

$$EPBT = \frac{\text{PV embodied energy} + \text{BOS embodied energy}}{\text{Annual PV system energy generation}} \quad (1)$$

Table 1. PV panel description.

PV type	Product name	Panel efficiency	Installed capacity (kWp)	Number of panels
Monocrystalline	mono-Si - SPR-MAX3-400	22.60%	2.8	7
Polycrystalline	poly-Si - JAP6-60-280/4BB/RE	17.12%	2.8	10
Cadmium telluride (CdTe)	CdTe - FS-6480A-C	19%	2.88	6
Copper indium gallium selenide (CIGS)	CIS - SF175-S - 175W	14.25%	2.975	17

To calculate the CPBT, One Click LCA was used to calculate the embodied carbon of each PV system. All the data used to calculate the embodied energy was also obtained from the One Click LCA database. A time horizon of 40, 25, 30 and 25 years was used for the monocrystalline, polycrystalline, cadmium telluride, and copper indium gallium selenide, respectively, which corresponds to the lifetime of each PV panel as specified by their manufacturers. The results of the net embodied carbon obtained from the One Click LCA software were then used to calculate the CPBT using Equations 2 and 3. For the CPBT, the PV panels' annual degradation was considered. The functional unit for comparing the CI of each PV technology is kWh.

$$\text{CPBT} = \frac{\text{PV system life cycle } CO_2\text{eq. emissions}}{\text{Avoided } CO_2 \text{ eq. emissions per year}} \quad \text{(2)(Muthu et al., 2014)}$$

Avoided CO_2 eq. emissions per year =

average yearly electricity of PV system × CO_2 eq. emission of the grid electricity (3)

3 Results and Discussion

3.1 Annual Electricity Generation

Table 2 shows the annual electricity generation per kWp for the monocrystalline and polycrystalline PV panels. Though the annual energy generation of the monocrystalline and polycrystalline are the same, the number of panels needed to generate the same amount of electricity from the polycrystalline PV panels was higher. The results confirmed that the annual electricity generation generally increases proportionally with the GHI, except for Akure, Ondo state, Nigeria, where less electricity was generated despite having a higher GHI than Helena, USA. Akure, Nigeria, has a very hot, humid climate, which causes an increase in the temperature of the PV panels, which reduces their performance. In Toledo, Spain, where the GHI is similar to Akure and the climate is not as hot, the annual electricity generation is higher than in Helena, USA.

Table 2. Annual electricity generation per kWp for monocrystalline and polycrystalline PV panels.

Country	Region	Coordinates	Climate	Best slope/azimuth	Annual electricity generation at best position (Mwh/kWp)	Annual electricity generation at horizontal position (Mwh/kWp)	Annual electricity generation at vertical south position (Mwh/kWp)	Annual electricity generation at vertical west/east position (Mwh/kWp)	Annual electricity generation at vertical north position (Mwh/kWp)
Norway	Steinkjer, Trøndelag	63.97°, 11.48°	6A-Cold - Humid	48/South	1.05	0.81	0.89	0.62	0.36
Canada	British Columbia	58.43°, -130.01°	7-very cold	44/South	1.37	1.06	1.14	0.81	0.44
United States	New York	43.11°, -76.10°	5A-Cool - Humid	33/South	1.47	1.31	1.05	0.84	0.48
United States	Helena	46.61°, -111.96°	6A-Cold - Humid	39/South	1.69	1.40	1.31	0.96	0.48
Spain	Toledo	39.88°, -4.05°	4B-Mixed - Dry	35/South	1.79	1.60	1.21	1.00	0.49

Nigeria	Akure, Ondo	7.25°, 5.20°	1A-Very hot -Humid	9/South	1.65	1.63	0.86	0.94	0.63
Australia	New South Wales	-31.53°, 145.80°	3B-Warm - Dry	30/North	2.01	1.82	0.53	1.11	1.32
China	Gar, Tibet	32.50°, 80.08°	7-very cold	35/South	2.28	2.03	1.63	1.41	0.74
Saudi Arabia	Najran	17.62°, 44.42°	1B-Very hot-dry	22/South	2.32	2.23	1.25	1.33	0.63
Chile	Calama	-22.47°, -68.90°	4C-Mixed - Marine	24/North	2.31	2.22	0.65	1.32	1.25

The highest amount of electricity is generated in the optimal position, followed by the horizontal position in most studied regions except Trøndelag, Norway and British Columbia, Canada, where the south orientation generates more electricity than the horizontal position because of their proximity to the north pole. As expected, in regions located further from the equator, in the northern latitudes, the south/north orientations generated more electricity than the west/east orientations. In regions closer to the poles, southern façades (for northern latitudes) and northern façades (for southern latitudes) are better for PV panel integration than horizontal roof-integrated PV panels. For regions closer to the equator, like Akure in Nigeria, Najran in Saudi Arabia, and Calama in Chile, the west/east orientations generated more electricity than the South and North orientations. Thus, when unobstructed, western and eastern façades are better for PV integration than southern and northern façades in regions closer to the equator. The electricity generated from cadmium telluride and copper indium gallium selenide PV systems follow the same trends in Table 2; however, they generated a little more electricity than the crystalline panels, mainly due to their slightly higher capacity.

3.2 Embodied Energy and Embodied Carbon of Different PV System Technology

According to IEA's methodological guidelines for PV systems, PV technologies should only be compared using the functional unit of kWh because each system's electricity may differ (Iea Pvps et al., 2020). The purpose of this section, therefore, is to describe the embodied energy and carbon of the different PV system technologies and not to provide a comparison of their environmental impact, which will be done in section 3.4. Table 3 shows the embodied energy and embodied carbon of the PV systems. Figure 2 shows the percentage contribution of the PV panel and BOS to the embodied energy and carbon. For the monocrystalline-based system, the PV panel is responsible for 38 per cent of the embodied carbon, but 89 per cent of the total embodied energy. The polycrystalline PV panel is responsible for 80 and 97 per cent of the embodied carbon and energy, respectively. For the cadmium telluride PV system, the panels account for 24 per cent of the embodied carbon and 78 per cent of the embodied energy. Copper indium gallium selenide PV panel accounts for 48 and 44 per cent of the embodied carbon and energy, respectively.

Table 3. Embodied energy and embodied carbon of the different PV systems.

	Embodied energy (MW)	Embodied carbon (kg CO_2e)
Monocrystalline (2.8kWp)	26.05	1838
Polycrystalline (2.8kWp)	53.30	3626
Cadmium telluride (CdTe) (2.88kWp)	14.79	1002
Copper indium gallium selenide (CIGS) (2.975kWp)	5.99	1440

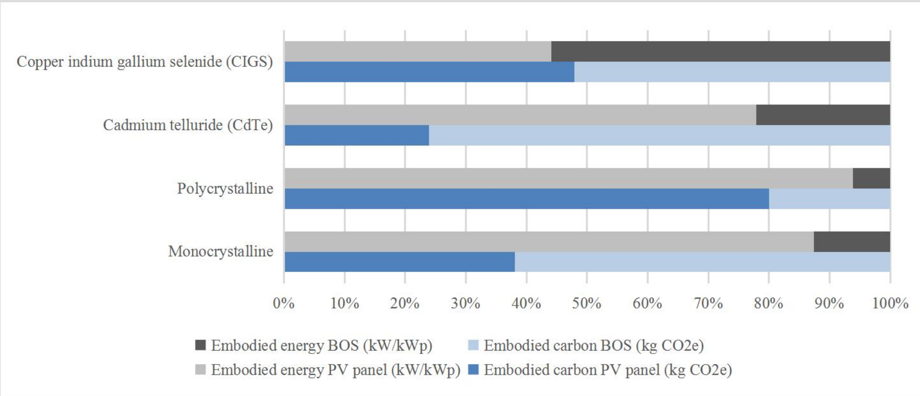

Fig. 2. Percentage contribution of the PV panel and BOS to the embodied energy and embodied carbon.

3.3 EPBT of PV System Technologies

EPBT of Monocrystalline PV System. In the optimal position, the EPBT for the monocrystalline PV system ranged from 2.4 years in Trøndelag, Norway, to 1.1 years in Calama, Chile (see Figure 2). As the annual electricity generated and GHI increased, the EPBT reduced. The EPBT of the façade with the least electricity generation in the studied regions was between 7.1 years in Trøndelag, Norway and 3.5 years in Tibet, China. The energy payback time for horizontal roof-integrated PV systems was between 1.2 and 3.2 years. For the west/east orientations, the EPBT was from 1.8 years in Tibet, China, to 4.2 years in Trøndelag, Norway. For the northern latitude regions, the longest EPBT occurred in PV systems positioned on the northern façade and for the southern latitudes, the longest EPBT was for PV systems placed on the south façade.

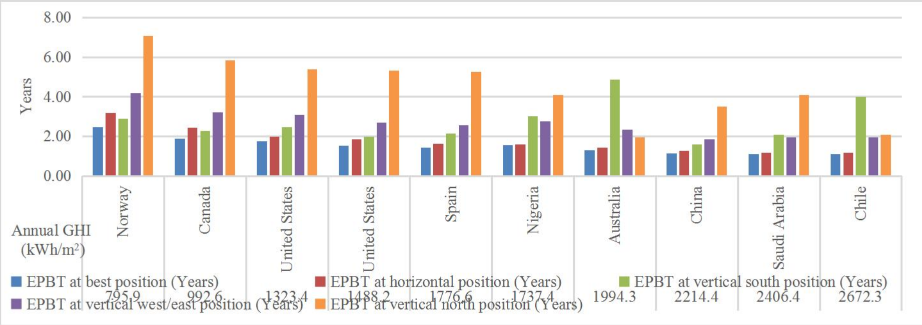

Fig. 3. EPBT of monocrystalline PV system.

EPBT of Polycrystalline PV System. While the annual electricity generated by the polycrystalline PV system is the same as that generated by the monocrystalline PV system, the number of PV panels and the length of structural support used in the polycrystalline PV system are more than those used in the monocrystalline PV system. Thus, the polycrystalline PV system requires a larger surface area. The general trend, as shown in Figure 3, shows that the EPBT of the polycrystalline PV system is more than that of the monocrystalline system. The primary reason for this difference is that the embodied energy of the polycrystalline PV panels and structural support are more than those of the monocrystalline PV system. In this system, for the optimal position, the shortest EPBT was 2.3 years in Najran, Saudi Arabia, while the longest EPBT was 5 years in Trøndelag, Norway. While in the worst position in the study regions, the EPBT ranged from 7.2 to 14.5 years in Tibet, China and Trøndelag, Norway, respectively. The EPBT was between 2.4 and 6.5 years for horizontal roof-integrated PV panels.

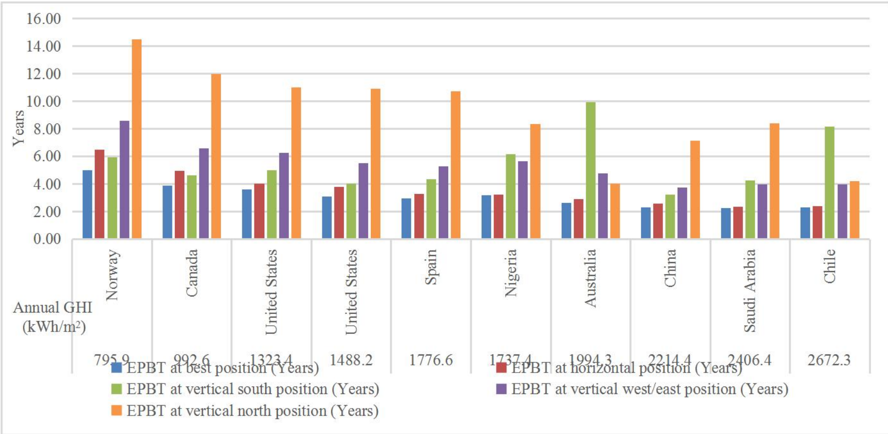

Fig. 4. EPBT of polycrystalline PV system.

EPBT of Cadmium Telluride PV System. Fig. 4 shows the EPBT of the cadmium telluride PV system. The EPBT in the optimal position was between 0.6 to 1.4 years in Najran, Saudi Arabia and Trøndelag, Norway, respectively. The EPBT of the cadmium telluride PV system is shorter than that of monocrystalline and polycrystalline PV systems. The shorter EPBT is not only due to the slightly higher electricity generation but mainly due to the lower embodied energy of the cadmium telluride PV panels. In the worst orientation, the EPBT for the study locations ranged from 2 years in Tibet, China, to 3.9 years in Trøndelag, Norway. The EPBT was between 0.6 and 1.8 years for the horizontal roof-integrated PV system.

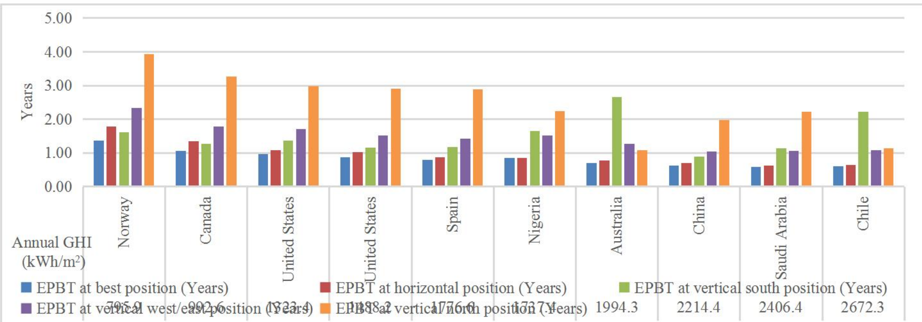

Fig. 5. EPBT of cadmium telluride PV system.

EPBT of Copper Indium Gallium Selenide PV System. The EPBT of the copper indium gallium selenide PV system is less than that of the monocrystalline, polycrystalline PV systems and cadmium telluride PV system. It also has the lowest embodied energy of all the four PV systems. From Fig 5, the EPBT of the copper indium gallium selenide PV system was between 0.3 and 0.5 years at the optimal position. While in the least optimal positions for the study regions, the EPBT was between 0.76 and 1.5 years in Tibet, China and Trøndelag, Norway, respectively. The EPBT for horizontal roof-integrated PV systems was from 0.3 to 0.7 years.

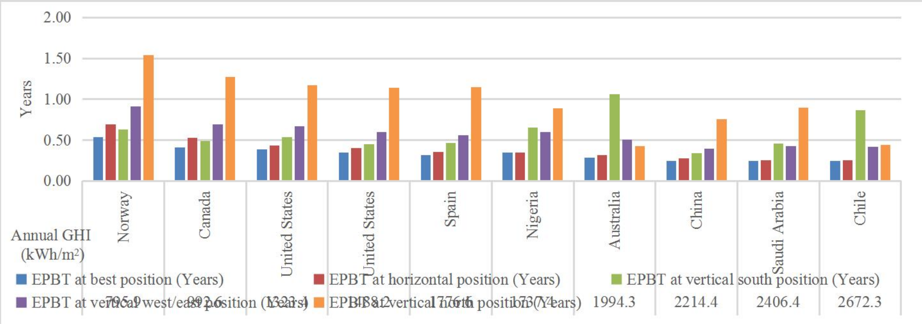

Fig. 6. EPBT of copper indium gallium selenide PV system.

3.4 CI and CPBT of PV System Technologies

CI of PV System Technologies. Table 1 shows the carbon intensity of electricity, CPBT and EPBT of different PV technologies in different regions and orientations. It was observed that the CI of the cadmium telluride PV system was the lowest of the four technologies, followed by that of the monocrystalline and then the copper indium gallium selenide PV system, respectively. The Polycrystalline PV system had the highest CI. The lifetime electricity generation and embodied carbon of PV systems influence their CO_2e emissions per kWh. Therefore, factors that influence the lifetime electricity generation of PV systems, like PV system components life span, panel efficiency and GHI, will influence the CI of electricity. The Monocrystalline PV system generates more electricity in its 40-year life span than the cadmium telluride PV system in its 30-year life span. Despite generating less electricity than the monocrystalline PV system, the cadmium telluride PV system has a lower carbon intensity because of its lower embodied carbon. The polycrystalline PV system and the copper indium gallium selenide have a life span of 25 years; however, the CI of the copper indium gallium selenide system is more than twice that of the polycrystalline system. The main contributor to the high CI of electricity generated from the polycrystalline PV system is its high embodied carbon.

The longer the service life of PV systems, the higher their lifetime electricity generation; which leads to a smaller CI. It is important to note that these results are peculiar to the specific PV panels used in this study; the outcomes might differ if PV panels from different manufacturers are used. The CI of the monocrystalline PV system was between 0.048 and 0.008 kg CO_2e /kWh in the worst and best electricity generation cases, respectively. The polycrystalline PV system's CI was between 0.156 and 0.025 kg CO_2e /kWh. The CI of the cadmium telluride PV system ranges from 0.034 to 0.005 kg CO_2e /kWh in the worst and best electricity generation cases, respectively. The CI for the copper indium gallium selenide PV system was between 0.056 and 0.009 kg CO_2e /kWh.

Table 4. Carbon intensity of electricity, CPBT and EPBT of different PV technologies in different regions and orientations.

				Mono-Si - SPR-MAX3-400 (2.8kWp, 7 number of panels, 22.6% efficient, 40 years life span)			Poly-Si - JAP6-60-280/4BB/RE (2.8kWp, 10 number of panels, 17.12% efficient, 25 years life span)			CdTe - FS-6480A-C (2.88kWp, 6 number of panels, 19% efficient, 30 years life span)			CIS - SF175-S - 175W (2.975kWp, 17 number of panels, 14.25% efficient, 25 years life span)		
Annual GHI (kWh/m²)	Location	National grid carbon intensity (kg CO_2e/kWh)	Orientation	Carbon intensity per kWh (kg CO_2e/kWh)	CO_2 eq. emissions PBT (years)	EPBT (years)	Carbon intensity per kWh (kg CO_2e/kWh)	CO_2 eq. emissions PBT (years)	EPBT (years)	Carbon intensity per kWh (kg CO_2e/kWh)	CO_2 eq. emissions PBT (years)	EPBT (years)	Carbon intensity per kWh (kg CO_2e/kWh)	CO_2 eq. emissions PBT (years)	EPBT (years)
795.9	Norway, Steinkjer, Trøndelag (63.97°, 11.48°)	0.03	Optimal	0.017	22.16	2.45	0.054	45.013	5.017	0.012	15.656	1.361	0.019	25.930	0.535
			Horizontal	0.022	28.77	3.18	0.070	58.437	6.512	0.015	20.419	1.775	0.025	33.532	0.690
			South	0.020	26.17	2.90	0.064	53.154	5.923	0.014	18.576	1.615	0.023	30.537	0.629
			West/east	0.028	37.88	4.19	0.092	76.934	8.573	0.020	26.814	2.331	0.033	44.237	0.911
			North	0.048	64.09	7.09	0.156	130.166	14.504	0.034	45.321	3.939	0.056	74.867	1.541
992.6	Canada, British Columbia (58.43°, -130.01°)	0.17	Optimal	0.013	3.02	1.89	0.042	6.130	3.871	0.009	2.134	1.052	0.015	3.532	0.413
			Horizontal	0.016	3.87	2.43	0.053	7.865	4.966	0.012	2.746	1.353	0.019	4.519	0.527
			South	0.015	3.61	2.26	0.050	7.333	4.630	0.011	2.572	1.267	0.018	4.209	0.491
			West/east	0.022	5.12	3.21	0.071	10.396	6.565	0.015	3.632	1.789	0.025	5.974	0.697
			North	0.040	9.34	5.85	0.129	18.970	11.978	0.028	6.620	3.261	0.046	10.904	1.272
1323.4	USA, New York (43.11°, -76.10°)	0.37	Optimal	0.012	1.29	1.76	0.039	2.626	3.600	0.008	0.902	0.965	0.014	1.521	0.386
			Horizontal	0.013	1.45	1.97	0.043	2.946	4.038	0.009	1.014	1.084	0.016	1.704	0.431
			South	0.017	1.81	2.46	0.054	3.668	5.028	0.012	1.276	1.364	0.019	2.110	0.534
			West/east	0.021	2.26	3.07	0.068	4.584	6.283	0.015	1.589	1.699	0.024	2.639	0.668
			North	0.036	3.95	5.37	0.118	8.022	10.994	0.026	2.780	2.972	0.043	4.618	1.169
1482.2	USA, Helena (46.61°, -111.96°)	0.37	Optimal	0.010	1.12	1.53	0.034	2.276	3.120	0.007	0.806	0.863	0.013	1.359	0.345
			Horizontal	0.013	1.36	1.85	0.041	2.757	3.779	0.009	0.951	1.017	0.015	1.596	0.404
			South	0.013	1.45	1.97	0.043	2.940	4.030	0.010	1.084	1.159	0.017	1.794	0.454
			West/east	0.018	1.98	2.70	0.059	4.024	5.516	0.013	1.420	1.519	0.022	2.361	0.598

			North	0.036	3.92	5.33	0.118	7.963	10.914	0.025	2.714	2.901	0.042	4.512	1.142
1776.6	Spain, Toledo (39.88°, -4.05°)	0.17	Optimal	0.010	2.25	1.45	0.032	4.574	2.956	0.007	1.553	0.783	0.012	2.665	0.319
			Horizontal	0.011	2.51	1.61	0.035	5.098	3.295	0.008	1.734	0.874	0.013	2.966	0.354
			South	0.014	3.33	2.14	0.047	6.770	4.375	0.010	2.332	1.176	0.017	3.910	0.467
			West/east	0.017	4.01	2.58	0.057	8.154	5.270	0.012	2.802	1.413	0.020	4.712	0.563
			North	0.036	8.19	5.25	0.116	16.630	10.748	0.025	5.713	2.880	0.042	9.608	1.147
1737.4	Nigeria, Akure (7.25°, 5.20°)	0.52	Optimal	0.011	0.81	1.57	0.035	1.652	3.210	0.007	0.554	0.840	0.013	0.967	0.348
			Horizontal	0.011	0.82	1.58	0.035	1.669	3.242	0.007	0.560	0.849	0.013	0.976	0.350
			South	0.020	1.56	3.01	0.066	3.175	6.167	0.014	1.085	1.644	0.024	1.835	0.658
			West/east	0.019	1.43	2.76	0.061	2.910	5.653	0.013	0.996	1.509	0.022	1.680	0.603
			North	0.028	2.12	4.09	0.090	4.302	8.358	0.019	1.474	2.234	0.032	2.482	0.891
1994.3	Australia, New South Wales (-31.53°, 145.80°)	0.55	Optimal	0.009	0.63	1.29	0.028	1.289	2.630	0.006	0.435	0.692	0.010	0.754	0.285
			Horizontal	0.010	0.70	1.42	0.031	1.427	2.911	0.007	0.482	0.767	0.011	0.833	0.314
			South	0.033	2.40	4.86	0.107	4.872	9.936	0.023	1.667	2.651	0.039	2.818	1.061
			West/east	0.016	1.15	2.32	0.051	2.330	4.752	0.011	0.797	1.268	0.019	1.348	0.508
			North	0.013	0.97	1.96	0.043	1.970	4.017	0.009	0.675	1.073	0.016	1.141	0.430
2214.4	China, Gar, Tibet (32.50°, 80.08°)	0.58	Optimal	0.008	0.53	1.14	0.025	1.074	2.322	0.005	0.373	0.628	0.009	0.621	0.249
			Horizontal	0.009	0.59	1.27	0.028	1.205	2.605	0.006	0.418	0.705	0.010	0.696	0.278
			South	0.011	0.74	1.59	0.035	1.501	3.245	0.008	0.529	0.892	0.013	0.860	0.343
			West/east	0.012	0.86	1.84	0.040	1.738	3.757	0.009	0.611	1.031	0.014	0.995	0.397
			North	0.024	1.63	3.50	0.077	3.314	7.164	0.017	1.166	1.967	0.028	1.897	0.758
2406.4	Saudi Arabia, Najran (17.62°, 44.42°)	0.71	Optimal	0.008	0.43	1.11	0.025	0.867	2.278	0.005	0.288	0.590	0.009	0.511	0.249
			Horizontal	0.008	0.44	1.16	0.026	0.902	2.369	0.005	0.300	0.614	0.009	0.531	0.258
			South	0.014	0.80	2.07	0.046	1.616	4.244	0.010	0.550	1.126	0.017	0.938	0.455
			West/east	0.013	0.75	1.95	0.043	1.518	3.987	0.009	0.517	1.058	0.016	0.879	0.427
			North	0.028	1.57	4.10	0.090	3.197	8.395	0.019	1.088	2.229	0.033	1.850	0.898
2672.3	Chile, Calama (-22.47°, -68.90°)	0.29	Optimal	0.008	1.04	1.12	0.025	2.114	2.285	0.005	0.718	0.606	0.009	1.229	0.246
			Horizontal	0.008	1.08	1.16	0.026	2.201	2.379	0.005	0.750	0.632	0.009	1.281	0.256
			South	0.027	3.71	3.98	0.088	7.541	8.151	0.019	2.643	2.228	0.032	4.351	0.869
			West/east	0.013	1.82	1.95	0.043	3.693	3.991	0.009	1.283	1.082	0.015	2.118	0.423

				North	0.014	1.93	2.07	0.046	3.913	4.229	0.010	1.346	1.135	0.016	2.234	0.446

(red)	Payback time greater than PV lifespan	(pink)	Payback time greater than 10 years

CPBT of PV System Technologies. Table 4 shows the CPBT and EPBT of the PV panels in different regions of varied GHIs; the areas in red show situations where the payback time is longer than the system's life span, while those in pink show where the payback time is more than ten years. Though there is no benchmark for the maximum EPBT and CPBT, ten years was chosen in this study as the cutoff point, beyond which PV installation is less advisable. The CPBT of PV systems in Steinkjer, Trøndelag, Norway, is higher than in all the studied locations. For the polycrystalline and the copper indium gallium selenide PV systems, which both have a life span of 25 years, embodied carbon cannot be offset. Monocrystalline and cadmium telluride PV systems have a life span of 40 and 30 years, respectively. When installed on the northern façade, their embodied carbon cannot be offset, while all the other orientations have a CPBT longer than 15 years. The main contributors to the long CPBT in Norway are the low GHI, which leads to lower electricity generation compared to the other study locations, and the low CI of Norway's grid electricity.

The factors that influence the CPBT include those that affect the electricity yield, the PV systems' CI, and the study location's grid electricity CI. From Table 4, it can be observed that the lower the CI of the PV system, the shorter the CPBT. The CPBT was as short as 0.4 years in Najran, Saudi Arabia, where the conditions favour high electricity yield, and the grid CI is very high, and as long as 64 years in Steinkjer, Trøndelag, Norway, for the monocrystalline PV system. For the cadmium telluride PV system, the shortest CPBT was 0.3 years in Najran, Saudi Arabia, and the longest was 45 years in Steinkjer, Trøndelag, Norway. For the polycrystalline PV system, the longest CPBT was 130 years in Steinkjer, Trøndelag, Norway, and the shortest was 0.9 years in Najran, Saudi Arabia. The results in Table 4 also emphasize that decisions on the sustainability of the PV systems cannot be made solely on EPBT alone. A PV system can have a short EPBT, which is observed in the copper indium gallium selenide PV system in Norway, but still has a very long CPBT.

3.5 Validation

Some of the assumptions and outcomes of this research were compared with the findings from previous research, though very few recent publications with installation scenarios similar to those used in this research exist. In the research by (Perez et al., 2012), the realistic EPBT for an 11.3 kWp façade integrated monocrystalline PV system (facing azimuth is 275°) was 3.8 years in New York. The results obtained from this research showed that for the façade integrated PV oriented to the west in New York, the EPBT is 3.1 years for a 3kWp capacity system, which is close to those obtained in (Virtuani et al., 2023) research. In the same study (Virtuani et al., 2023), the CI of PV systems in Norway for the optimal position was 0.045 kg CO_2e /kWh, which is close to the 0.054 kg CO_2e /kWh obtained for the polycrystalline PV system used in our study. According to (Virtuani et al., 2023), the CI for Spain in the optimal placement was 0.026 kg CO_2e /kWh, while that in this study was 0.032 kg CO_2e /kWh for the polycrystalline PV system. Data form the above publications were deemed comparable with the ones in this study.

4 Conclusion

This research set out to determine the EPBT, CPBT and CI of four PV system technologies (3kWp capacity) for ten study locations, assuming that they are installed at the optimal position, horizontally integrated into the roof and vertically on the façades facing the four cardinal points. The findings of this research show how different PV panel orientations influence the EPBT. In all the study locations and orientations, the EPBT was reached within the lifetime of the PV panels. However, the PV systems on the northern façade of five study locations in the polycrystalline PV system were over ten years old. It was also observed that the EPBT was not sufficient to decide on the environmental viability of PV systems. Although Steinkjer, Trøndelag, Norway had an EPBT ranging from 2.5 to 14.5 years, the CPBT was above 20 years in most PV system types and orientations. Based on this finding, the analysed BIPV systems are not environmentally advisable in Norway. For all the other study regions, however, most of the EPBT and CPBT are less than ten years and frequently below five years. In this study, the CI of four PV system technologies were also compared; the results indicated that the cadmium telluride PV system had the lowest CI, followed by the monocrystalline and the copper indium gallium selenide PV system, respectively.

5 Limitations and Contribution to Knowledge

This research was conducted to bridge the gap identified in BIPV LCA research, where limited publications were available on the EPBT, CPBT and CI of different BIPV technologies. Also, recent review publications on BIPV LCA largely compiled findings from research published more than five years ago. Many publications mainly examined only one of the three parameters (EPBT, CPBT and CI) in this study. The EPBT, CPBT and CI of four BIPV technologies were calculated in ten locations with different GHI and grid electricity CI in various orientations, illustrating how the solar energy potential (GHI) and CI of grid electricity influence the environmental viability of BIPV projects. One of the limitations is that the analysis did not capture the cost feasibility of the various BIPV scenarios examined, which would also require a broader investigation outside the scope of the present study, including local policies, market characteristics, fiscal regimes, public incentives and more. This offer ground for further research. Assessing the economic viability of BIPV systems in the study regions and orientations will further aid all the relevant stakeholders in the decision-making process. Another limitation of this study is the focus on only four PV technologies due to the limited availability of data (EPDs). Nonetheless, the study provides a dataset representative of a comprehensive range of technologies and environmental conditions, providing valuable information for the planning of BIPV systems.

References

1. Global Solar Atlas 2.0. (2020). Global Photovoltaic Power Potential by Country. A Free, Web-Based Application Developed and Operated by the Company Solargis s.r.o. on Behalf of the World Bank Group, Utilizing Solargis Data, with Funding Provided by the Energy Sector Management Assistance Program (ESMAP).
2. González-Torres, M., Pérez-Lombard, L., Coronel, J. F., Maestre, I. R., & Yan, D. (2022). A review on buildings energy information: Trends, end-uses, fuels and drivers. Energy Reports, 8, 626–637. https://doi.org/10.1016/j.egyr.2021.11.280
3. Iea Pvps, Frischknecht, R., Stolz, P., Heath, G., Raugei, M., Sinha, P., & de Wild-Scholten, M. (2020). Methodology Guidelines on Life Cycle Assessment of Photovoltaic Electricity. https://doi.org/10.13140/RG.2.2.15574.88648
4. JA SOLAR. (2019). JAP60S09 280/SC (JASO-00004-V01.01-FR) [Dataset].
5. Kant Paliwal, M., Jakhar, S., & Sharma, V. (2024). A bibliometric and scientific mapping of the research landscape and trending topics in building integrated photovoltaic systems. Solar Energy, 267. https://doi.org/10.1016/j.solener.2023.112202
6. Muteri, V., Cellura, Curto, D., Franzitta, Longo, S., Mistretta, & Parisi, M. L. (2020). Review on Life Cycle Assessment of Solar Photovoltaic Panels. Energies, 13, 252. https://doi.org/10.3390/en13010252
7. Muthu, M., Victor, K., & Rajasekaran, R. (2014). Energy pay back period and carbon pay back period for solar photovoltaic power plant. International Journal of Chemical Sciences, 12, 293–305.
8. Perez, M. J. R., Fthenakis, V., Kim, H. C., & Pereira, A. O. (2012). Façade-integrated photovoltaics: A life cycle and performance assessment case study. Progress in Photovoltaics: Research and Applications, 20(8), 975–990. https://doi.org/10.1002/pip.1167
9. Stamford, L., & Azapagic, A. (2019). Environmental impacts of copper‐ indium‐ gallium-selenide (CIGS) photovoltaics and the elimination of cadmium through atomic layer deposition. Science of The Total Environment, 688. https://doi.org/10.1016/j.scitotenv.2019.06.343
10. SunPower. (2021). MAXEON 3 MONO-CRYSTALLINE PHOTOVOLTAIC MODULE (NEPD-3087-1726-EN) [Dataset].
11. United Nations Department of Economic and Social Affairs, Population Division. (2022). World Population Prospects 2022: Summary of Results. UN DESA/POP/2022/TR/NO. 3.
12. Virtuani, A., Borja Block, A., Wyrsch, N., & Ballif, C. (2023). The carbon intensity of integrated photovoltaics. Joule, 7(11), 2511–2536. https://doi.org/10.1016/j.joule.2023.09.010
13. von Malmborg, F. (2024). Strategies and Impacts of Policy Entrepreneurs: Ideology, Democracy, and the Quest for a Just Transition to Climate Neutrality. Sustainability, 16, 5272. https://doi.org/10.3390/su16125272
14. Wikoff, H., Reese, S., & Reese, M. (2022). Embodied energy and carbon from the manufacture of cadmium telluride and silicon photovoltaics. Joule, 6. https://doi.org/10.1016/j.joule.2022.06.006